DIAGNOSIS OF ANOMALOUS PATTERNS OF PRECIPITATION IN NORTH CHINA AND CLIMATIC PREDICTION EXPERIMENTS

YOU Fengchun (尤凤春)[1], *DING Yuguo* (丁裕国)[2], *ZHOU Yu* (周 煜)[3]

and *SHI Yinshan* (史印山)[1]

1. Weather Center of Hebei Province, Shijiazhuang 050021
2. Nanjing Institute of Meteorology, Nanjing 210044
3. China Meteorological Administration, Beijing 100081

Received November 28, 2001; revised May 30, 2002

ABSTRACT

In the context of 1965 — 2000 monthly rainfall data from 73 stations distributed over 3 province-level districts and 2 metropolises (Beijing and Tianjin) of North China with some stations in the neighboring provinces, diagnostic study is undertaken of the features of spatially anomalous patterns and dominant periods of the annual precipitation in terms of EOF, REOF and SSA. Also, a scheme consisting of SSA combined with autoregression (AR) as a prediction model is employed to make forecasts of monthly rainfall sequences of the anomalous patterns in terms of an adaptive filter. Results show that the scheme, if further improved, would be of operational utility in preparing county-level prediction.

Key words: anomalous pattern, singular spectral analysis, autoregression model (AR model), short-term climate prediction

I. INTRODUCTION

North China is one of the economically advanced regions of China, covering about 8.5% of the land territory with a range of landforms consisting of plains, plateau, a chain of basins and mountainous/hilly land. The climate there differs greatly from place to place and so does its variation because of vast difference in elevation between the different kinds of terrain, higher latitudes and pronounced discrepancy in distance from the sea—all these make North China a "climatically sensitive area". Data made over the past decades show that flood and persistent drought events as climate disasters have frequently hit this area, impinging seriously upon its political, economic and social prosperity. Many studies have been devoted to rainfall features on a national basis (Huang 1988b; 1991; Chen 1991; Zhang 1993) and some efforts have been made to address these disasters of some parts of the country using still fuller data (Li 1992; Li et al. 1997; Sun et al. 2000). However, relatively fewer articles have been published that deal with rather detailed diagnosis and prediction of anomalous patterns of North China precipitation. Techniques of principal components PCs, and rotated principal components (RPCs) and SSA (singular spectral analysis) are employed in this paper to diagnose the characteristics of extraordinary rainfall patterns on an annual basis (January — December) and their respective leading quasi-oscillatory periods in the context of 1965 — 2000 monthly rainfall data from 73 stations over North China and its thereabouts with the aim at gaining further insight into the climate-related abnormal rainfall patterns. Obviously, our study is of great significance to the exploration of the causes and development of prediction techniques. Furthermore, based on the diagnostic findings, predictions of sequences of monthly rainfall anomaly for all the patterns are made in terms of an adaptive filter with the aid of SSA and AR model in combination.

II. DATA AND METHOD

The data of 1965 — 2000 monthly rainfall came from 73 representative stations covering the study region and its vicinity. To get rid of effects of the geographic position, topographic features and yearly variation, these data were normalized, resulting in the standardized data matrix $(X_{ji})_{mn}$ where the station number $j=1, 2, \cdots, m$ $(m=73)$ and annual sample number $i=1, 2, \cdots, n$ $(n=36)$. The data matrix ${}_mX_n$ is decomposed in the following way. The matrix takes the form

$$ {}_mX_n = {}_mV_k \begin{bmatrix} \sqrt{\lambda_1} & & & 0 \\ & \sqrt{\lambda_2} & & \\ & & \ddots & \\ 0 & & & \sqrt{\lambda_k} \end{bmatrix} \begin{bmatrix} 1/\sqrt{\lambda_1} & & & 0 \\ & 1/\sqrt{\lambda_2} & & \\ & & \ddots & \\ 0 & & & 1/\sqrt{\lambda_k} \end{bmatrix} {}_kT_n = {}_mL_k\, {}_kF_n, \tag{1} $$

where $L_{(m\times k)}$ denotes a matrix of space load vectors (LVs), $F_{(k\times n)}$ the matrix of principal components and λ_j the eigenvalue of a matrix of correlation coefficients $R_{(m\times n)}$ of $X_{(m\times n)}$. To make clearer a feature of a rainfall distribution for revealing its main characteristics, we adopted a scheme of maximum-variance RPCs for treating EOF-given LVs and their PCs, viz. , multiplying the LVs matrix L and (PCs matrix F) by an orthogonal matrix $\Gamma(\Gamma')$ on the right (left) hand side (Horel 1999). The procedure for such paired rotations is repeated one by one, leading to

$$ B = L\Gamma, \qquad G = \Gamma' F, $$

where B and G stand for rotated load vectors (RLVs) and the related rotated PCs (RPCs). For the principles of maximum-variance RPC analysis the reader is referred to Huang (1988b) and Shi (1995).

On the other hand, by applying SSA to a timeseries x_t (with $t=1, 2, \cdots, n$) to make it arrange on a time lag scale m, we have

$$ X = \begin{bmatrix} x_1 & x_2 & \cdots & x_{n-m+1} \\ x_2 & x_3 & \cdots & x_{n-m+2} \\ \cdots & \cdots & \cdots & \cdots \\ x_m & x_{m+1} & \cdots & x_n \end{bmatrix} = (x_{it})_{m\times(n-m+1)}. \tag{2} $$

Then the matrix X is EOF expanded, resulting in an expanded time empirical orthogonal functions (TEOFs). As shown in Ding et al. (1998), SSA is proved theoretically to be TEOF, which is essentially "generalized power spectral analysis". SSA functions as a means of extracting x_t contained wave pattern signals out of a noise system, and by decomposing the associated TPCs (time PCs) we identify signals of the leading periods such that we get one-type signal for one-type period from noise background, and such signals are examined together with time variation of related TPCs at different intervals to reveal their time-varying features. On this basis, we are permitted to reconstruct series of components (denoted as RCs) for each of the signals marked by one-kind frequency with the aid of TPC and TEOF components. Not only does the RC reconstruction transform the recognition of frequency periods into that of temporal periods but the diagnosis of timeseries-contained signals of periods at differing intensity is converted into a problem of prediction as well. RCs here have the form

$$X_t^{(k)} = \begin{cases} \dfrac{1}{m}\sum\limits_{i=1}^{m} L_i^k a_{t-i+1}^k & m \leqslant t \leqslant n-m+1, \\ \dfrac{1}{t}\sum\limits_{i=1}^{t} L_i^k a_{t-i+1}^k & 1 \leqslant t \leqslant m-1, \\ \dfrac{1}{n-t+1}\sum\limits_{i=t-n+m}^{m} L_i^k a_{t-i+1}^k & n-m+2 \leqslant t \leqslant n, \end{cases} \tag{3}$$

where L_i^k is the ith phase component of the kth typical wave pattern and a_{t-i+1}^k represents the $(t-i+1)$-th value of the kth PC. Then $X^{(k)}$ signifies a reconstructed sequence of the kth component, denoted normally as RCs-k.

The first p pronounced wave patterns or periodic components are used to reconstruct primitive sequences, which take on the approximate form

$$X_t \approx \widetilde{X}_t = \sum_{k=1}^{p} X_t^{(k)}. \tag{4}$$

The use of SSA in combination with AR as a prediction model allows to establish a lower-order AR (p) model through RCs-k based upon of SSA-decomposed TPCs. With the AR (p) model, extrapolative prediction of all components could be performed, finally arriving at synthetic prediction.

III. CLASSIFIED ANOMALOUS RAINFALL PATTERNS AND THEIR FEATURES

The rainfall fields are delimited by LVs and RLVs from RPC study of the element for the project area. Results suggest that RPCs make percentage contributions to total variance of the field that are more uniformly scattered compared to PCs and the order of percentages is changed for some PCs, thereby bringing out physical implication more clearly i. e., the features of space correlativity (RPCs vs PCs) and for each of the components, its associated space pattern allows its total variance contributions to be concentrated in a related pattern as much as possible and minimizes such contributions in other regions. This serves the purpose of objective categorization of precipitation patterns.

From the percentage contributions of PCs and RPCs to total variance of the study patterns we see that the convergence becomes slowed down of these fields with the extension of space/time scales and increase in the number of stations. This illustrates quite well that the project region is marked by great differences on a space/time basis for its different parts because of its vast expanse and complicated topography. As a consequence, it is worthwhile to undertake a study in detail of the spatially abnormal

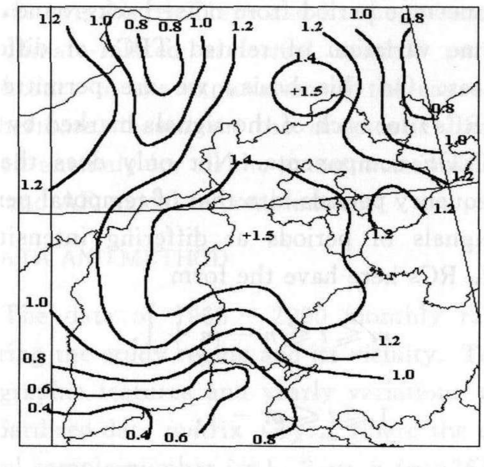

Fig. 1. Distribution of the first LV (× 10) (denoted as LV1) of annual precipitation in North China.

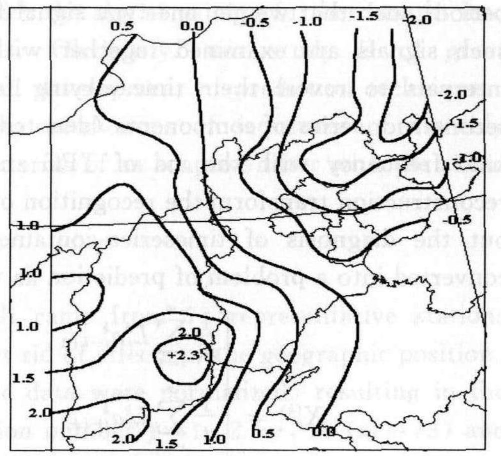

Fig. 2. As in Fig. 1, but for the second LV (dnoted as LV2).

Table 1. Percentage Contributions of the First Eight PCs and RPCs to Total Variance for North China

Number	1	2	3	4	5	6	7	8
PC	33.9	11.8	8.7	6.3	4.5	4.1	3.4	2.7
RPC	12.8	7.0	9.4	7.1	3.4	8.5	4.4	2.5

structures. Table 1 summarizes PC and RPC contributions in percentage to total variance of the rainfall field of North China.

Figures 1—3 present the distributions of the first three LVs (×10), signifying a full picture of the spatially abnormal structures of North-China rainfall on an annual basis.

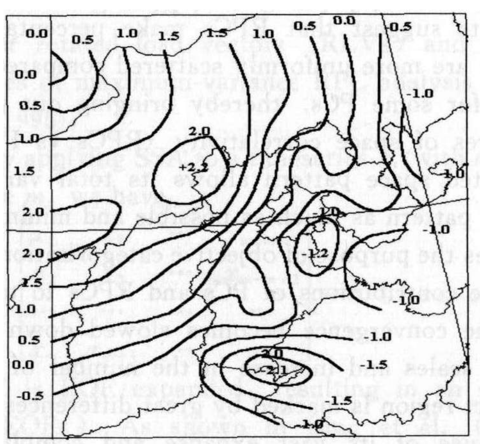

Fig. 3. As in Fig. 1, but for the third LV (denoted as LV3).

Viewed from Fig. 1, LV1 shows its positive values all the region over, suggesting consistency throughout and that the pattern accounts for 33.9% of total variance, which is obviously related to effects of large-scale weather systems. This implies that despite great difference climatically in the whole region, annual rainfall is, to some extent, under the joint effect and control of several factors. We notice that maximum LV1 band is in the middle part, with the central magnitude reaching 0.15, which means that this segment is marked by larger variability of rainfall in North China and extremely sensitive to the anomaly of floods and droughts.

Looking at LV2 distribution of Fig. 2, we see a "southern positive-northern negative" pattern, which makes up 11.8% of total variance, i.e., positive values are distributed in much of Shanxi Province and southwest Hebei, centered at south Shanxi with a central value of 0.23, and negative values are in the east and north of Hebei Province, central and eastern Inner Mongolia, centered on southeast Inner Mongolia.

From LV3 distribution we notice a pattern with western negative and eastern positive values that accounts for 8.7% of total variance, with the zero line running from NW Hebei to southern Shanxi, a positive-value belt to the west that is centered (0.22) at the borders between Inner Mongolia, Shanxi and Hebei, and a negative belt in eastern North China centered (−0.21) on the borders of Hebei, Henan and Shandong Provinces.

The anomalous patterns of annual precipitation include a positive-value distribution almost throughout North China (LV1), the opposites in the south vs north (LV2) and east vs west (LV3). To make climate features of the yearly rainfall clear on a local basis we perform rotation of load vectors associated with the first 8 principal components and we get 5 leading spatially anomalous patterns from the first 6 but the fifth RLV fields.

Figure 4a depicts that RLV1 high-value band is in eastern North China (whose information comes dominantly from LV3) with the central value of 0.7 located in Beijing, Tianjin and the vicinity of the seaboard, and the magnitude is much bigger than before rotation, referred to as an Eastern North-China Pattern. This pattern-covered area has greater mean of yearly rainfall with moderate variability in the averages. This situation makes this portion a particular precipitation pattern.

Figure 4b presents the RLV2 distribution with a high-value band in southern North China and the central value of 0.7 is a lot bigger than before rotation. The distribution has its information largely from LV2 and is called a Southern North China Pattern. It is worth mentioning that this pattern covers a region with maximum rainfall variability in the project area where most of the annual precipitation is often provided by a few rainstorms and 70%−80% of yearly rainfall occurs in summer (Hebei 1990), e.g., the events observed in August 1963, August 1996 and July 2000, thus making rather distinct its regional features of flood and drought.

The RLV3 field has its high-value band positioned in western North China., viz., from western Shanxi to central Inner Mongolia, with the information coming mainly from LV3. It is named a Western North China Pattern, whose central value reaches 0.9. This pattern receives less rainfall on an annual basis but shows greater variability.

The northern part of North China is another extraordinarily sensitive region, especially the band from northern Hebei to eastern Inner Mongolia. This is called a

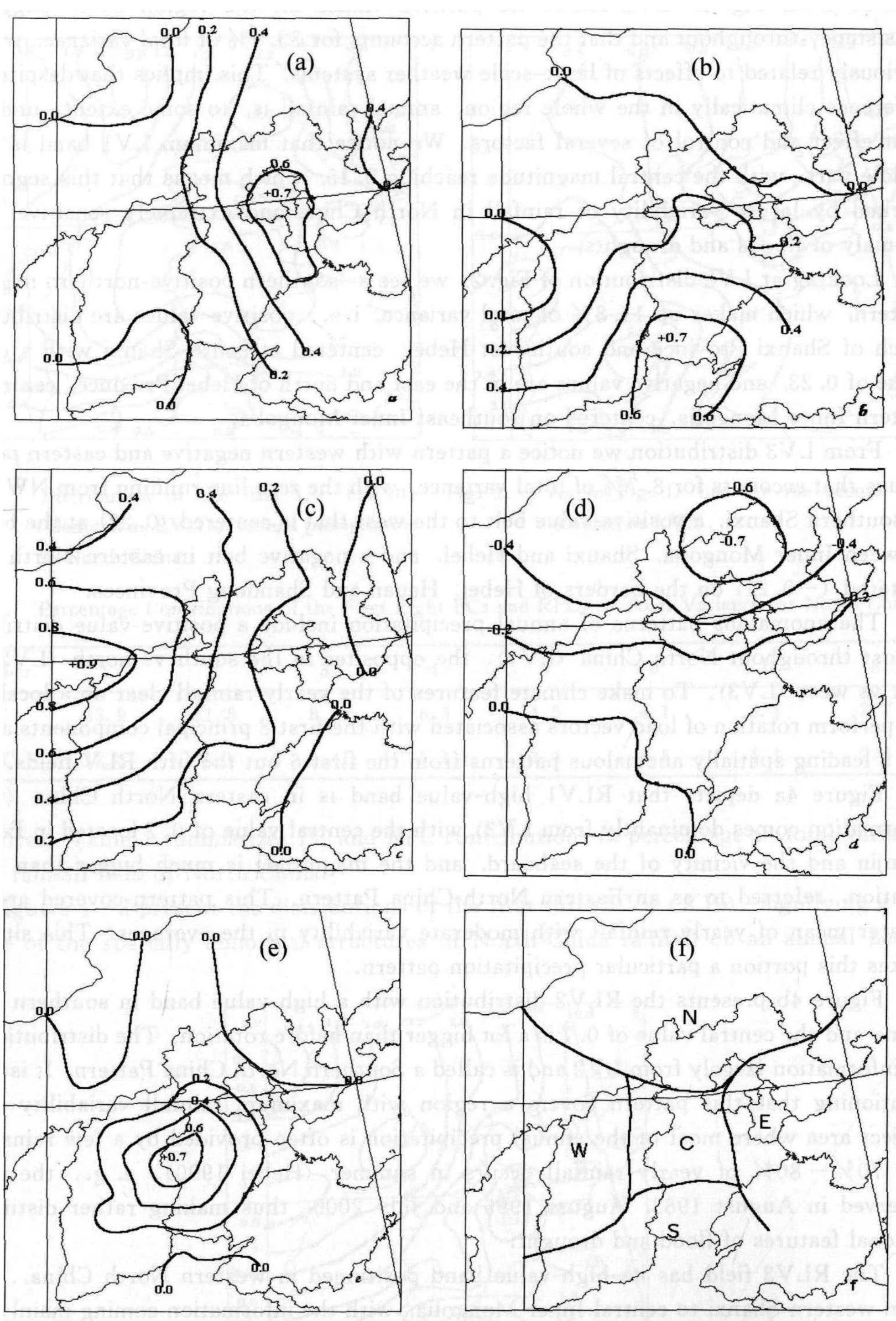

Fig. 4. The 1st RLV field of annual precipitation in North China for (a) RLV1, (b) RLV2, (c) RLV3, (d) RLV4, (e) RLV6, and (f) main patterns of spatially anomalous rainfall in North China.

Northern North China Pattern (Fig. 4d of RLV4, whose information comes dominantly from LV2), with the central value of −0.7 in the northern portion of North China. This pattern represents all mountainous climatic features with minimum annual mean and variability, meaning that its basic feature is dry.

Viewed from Fig. 4e for the Central North China Pattern, the high-valued RLV6 band lies in middle North China, centered (as much as 0.7) around the middle part of the Taihang Mountains, with information largely from LV1. Within this region the mean and variability are rather big such that it is an area often hit by torrential rain and severe drought.

The principle of separating rainfall patterns consists in the similarity of station rainfall variation for a particular pattern and in great difference in rainfall variation between stations in different patterns. Any of the rainfall patterns consists of neighboring stations with load$\geqslant$0.5 in the same LV field. However, some stations may be put into two or more neighboring patterns and fall into the one with maximum load of the LV field. As a result, station rainfall means within the same pattern have analogous variations. The delimited patterns are shown in Fig. 4f.

The five patterns of abnormal precipitation in the project region are an Eastern, a Southern, a Western, a Northern and a Central North China Pattern, which is very close to the regionalization from cluster analysis. It follows that the climate rainfall prediction, if made successfully, allows to get the key kind of annual anomaly for this study region.

IV. SSA-GIVEN LEADING PERIODS OF THE PATTERNS

SSA (singular spectral analysis) is regarded as a technique especially suitable for investigating periodic oscillation (Vautard 1992). For the patterns obtained, their temporal coefficients are SSA examined, separately, in order to explore properties of signals of quasi-periodic oscillations for each of the patterns to gain a fuller picture of the periods, thus providing with basis for short-range climate prediction.

Generally, the bigger the maximum time lag M, the more sensitive the spectral resolution. Tests show that if the window length is M, we can well identify oscillations at periods of $M/5-M$ but M should not exceed $N/3$ so as to make statistical error of an estimate from cross covariance of maximum time lag $M-1$ bigger than the estimate itself. The used data cover 1965−2000 (the sample size is $n=36\times12$). This allows to take $M=$ 110 months, which ensures $M<N/3$ and makes spectral resolution rather sensitive as well. Besides, experiments were conducted with $M=100$, 120 and 130 months, separately, indicating no big variation.

The distributions of the first eight eigenvectors (typical wave-pattern vectors) are given by SSA (figure not shown), giving dominant period modes for each of the rainfall patterns.

Table 2 presents the percentage contributions to total variance for the first eight eigenvalues from SSA, which differ in magnitude, with maximum sum for the Southern Pattern (85.9%), next for the Western (82.8%) and minimum for the Northern (70.7%). Hence, we can see that the modes of the leading periods are well denoted by signals contained in the 8 eigenvalues for the Eastern Pattern and those in the first 6 eigenvalues for the other 4 patterns can do so, too, because their totals reach, in order, 76.2%, 72.0%, 61.9% and 64.5% for the Southern, Western, Northern and Central Patterns.

Table 2. Contributions (in %) to Total Variance of the First Eight SSA Eigenvectors (the Nested Dimension is 110 Months) for the Five Rainfall Patterns Demarcated, Denoted by E, S, W, N and C

	1	2	3	4	5	6	7	8	Total
E	16.5	15.4	12.7	10.7	8.5	7.3	4.4	3.9	79.4
W	15.9	15.2	11.4	11.0	9.8	8.7	5.5	5.3	82.8
N	16.3	15.5	9.4	8.4	6.5	5.8	4.9	3.9	70.7
S	17.3	16.7	12.3	11.5	9.8	8.6	5.2	4.5	85.9
C	17.4	16.3	10.8	9.9	5.4	4.7	4.1	3.8	72.4

Following Vautard (1992), we can extract from the first 6 to 8 eigenvalues out of these patterns, depending on circumstances, 3—4 kinds of signals of significant periodic oscillations, which are shown in Table 3.

Table 3. SSA-Given Signals of Pronounced Periods for the Rainfall Patterns, Briefly Denoted by E, S, W, N and C, and M Standing for Months

	$TC_{1,2}$	$TC_{3,4}$	$TC_{5,6}$	$TC_{7,8}$
E	85—95 (M)	50—60 (M)	30—36 (M)	22—26 (M)
S	22—26 (M)	50—60 (M)	30—36 (M)	
W	22—26 (M)	30—36 (M)	85—95 (M)	
N	22—26 (M)	50—60 (M)	30—36 (M)	
C	22—26 (M)	85—95 (M)	30—36 (M)	

Table 3 shows that the periodic signals contained in these patterns somewhat differ. Nevertheless, the most dominant periods are analogous for all but the Eastern Pattern, with their eigenvectors 1 and 2 indicative of quasi 2-year periods versus the quasi 7—8 year oscillations for the Eastern Pattern whose eigenvectors 7 and 8, however, signify quasi 2-year oscillations. The second remarkable periods of all except for the Western Pattern are quite noticeably long, e. g., the Central Pattern has quasi 7 — 8 year periods, the Southern, Northern and Eastern Patterns display quasi 4—5 year oscillations compared to quasi 3-year periods for the Western Pattern. The third remarkable periods are shortened, mostly to quasi 3 year oscillations, the exception being the Western Pattern of quasi 7—8 year oscillations. The findings presented here are in agreement with the power spectral analysis of the quasi 2—7 year periods for the valleys of the Haihe River in the east part of North China (Tang et al. 1990).

The variations in these oscillatory components are varied for these rainfall patterns, thus leading to complicated properties of annual precipitation in North China. Based upon their respective variation in the components, however, regression analysis can be made for extrapolative prediction for each pattern.

V. EXPERIMENT ON SHORT-RANGE CLIMATE PREDICTION OF THESE PATTERNS

To raise predicting accuracy a scheme of SSA and AR (auto-regression) in combination is developed to predict the rainfall for these patterns in terms of an adaptive filter. By means of the SSA and AR scheme Ding (1998a) conducted successfully experiments on short-range prediction of the Nino-region SSTA intermonthly mean series. But experiments on rainfall prediction are relatively fewer. Short-term prediction of monthly anomaly sequences for these patterns dealt with in the present study provides a new approach to precipitation research.

1. *Data and Preprocessing*

The 1965—2000 monthly rainfall data of each study station in North China and its neighborhood constitute a timeseries that is normalized. It should be noted that the monthly sequences standardized by regionally averaged rainfall contain undamaged multi-frequency signals thereof so as to keep oscillatory information inside at periods, intraseasonal, seasonal and interannual. There were studies performing such prediction in the context of an interannual series with a month fixed. As a result, this practice is undoubtedly responsible for the loss of part of useful signals, which is unacceptable even in the research of periods at interannual oscillations. This would not lead at least to the full utilization of the interactions between the oscillations on differing scales, seasonal and intraseasonal, for example. Viewed from sampling, pieces of information in intermonthly series are in closer conformity to the requirement of frequency signals sampling theorem so as to reduce the frequency "confusion" (Priestley 1981)

2. *Construction of an SSA-AR (p) Model with Its Experiment*

SSA is applied to the data series of all the patterns, leading to TPC components, followed by Eq. (3) —reconstructing the series RCs for a lower-order AR (p) model, thereby permitting to make extrapolative prediction of the components. Then Eq. (4) is employed to make superimposition of extrapolative sequences in order to prepare prediction, in terms of an adaptive filter, of the rainfall inside the patterns. The procedure is 1) preprocessing of the series of each of the patterns; 2) the SSA treatment of timeseries; 3) reconstruction of RCs for each of the patterns; 4) establishment of an AR model from the RCs for each of the patterns to make extrapolative prediction; and 5) synthesis of the extrapolative prediction series for final result.

An attempt was made to prepare an AR model from reconstructed RCs 1—8 related to TCP1 — 8 for each pattern in the interval of January 1965 — December 1998, with the optimal number of order p selected from the RCs by means of FPE criterion. The p is somewhat different from one pattern to another, varying normally between 1 and 5. Results suggest that most of the RCs are suitable for the establishment of a lower-order AR model with quite good fitting. Besides, because the prepared model is simple in structure and the contained signals are too simple to be interfered by strong noise, extrapolative prediction is founded on solid basis.

Experiments are performed in terms of different maximum time lag M, with the

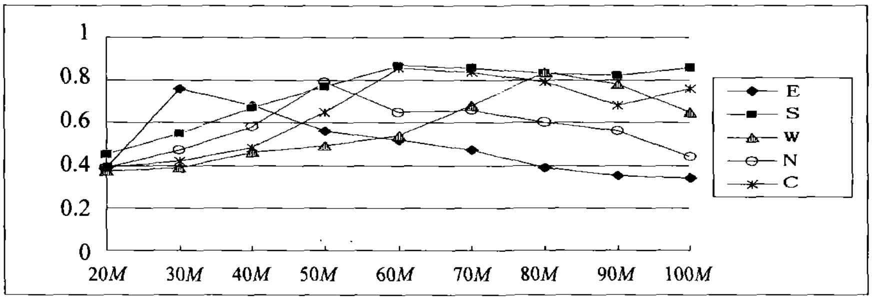

Fig. 5. The fit of correlation coefficients between the predictions and measurements for the rainfall patterns at a range of maximum time lag M, where E, S, W, N and C standing for the Eastern, Southern, Western, Northern and Central Patterns, respectively.

results given below.

It is apparent from Fig. 5 that different values of M have effect on the fittings for the patterns, and only for an appropriate M is higher fit possible. For this reason, M of 30, 60, 80, 50 and 60 are suitable, respectively, for the Eastern, Southern, Western, Northern and Central Patterns in the study region.

Predictions were made by use of monthly series as independent samples covering January 1999 to December 2000, indicating rather good agreement between the predicted and observed values (figure not shown). We get the correlation of 0. 84 between the superimposed and predicted series for the Central Pattern. However, if the fit and prediction were made by the AR (p) model based directly upon primitive sequences, results would not be so good. Take for example the Central Pattern. The AR (p) model-given fit and prediction show the correlation coefficient of as low as 0. 38 between predicted and measured values for January 1999 to December 2000, indicating that the AR (p) prediction without SSA treatment produces poor evidence. However, it is worth noting that low-pass filtering has, in effect, been made of primitive sequences in the SSA-AR scheme, leading to TPC1 — 8 making up 72. 4% of total variance. Evidently, the higher prediction of 0. 84 should, in fact, be approximately a — 61% accuracy predicted by primitive series — the accuracy refers to the variance contribution sum of SSA-given first 8 eigenvectors multiplied by the correlation coefficient between the superimposed and predicted series (0. 84 × 0. 72) — plus about 0. 23 improvement through the comparison made in order with the AR (p) results. Evidently, our SSA-AR model shows its improvement of 23% compared to 38% accuracy just from the AR (p) model. In other words, the background noise inherent in the primitive sequences has been removed in the filtered series, resulting in nearly 23% improvement of the prediction. This demonstrates merits of the SSA-AR scheme.

Likewise, we get predictions for the other patterns, as shown in Table 4, wherefrom we notice that as regards the fit and prediction the SSA-AR is superior to the AR (p) model in the improvement of as high as 40% of rainfall prediction for the Southern Pattern compared to 16% only for the Northern equivalent just based on the AR (p).

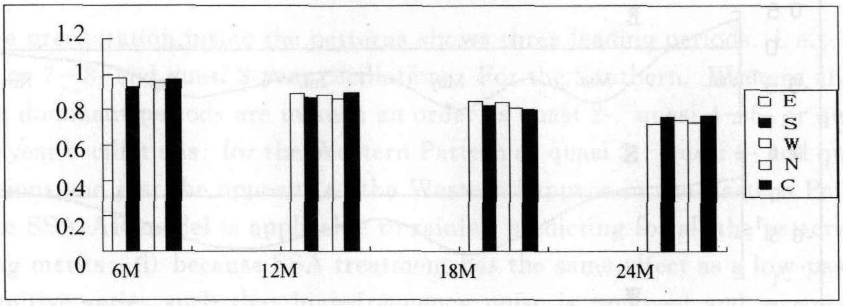

Fig. 6. Correlation coefficients between prediction and measurement for all the patterns, with the blocks arranged rightward denoting, in order, the Eastern (E), Southern (S), Western (W), Northern (N) and Central (C) Patterns. M standing for months.

Table 4. Predictions of Precipitation in the Five Patterns

	SSA-AR model			AR (p)	Improvement
	TPC1−8	correl.	APSP*		
E	79.4%	0.72	0.57	0.30	0.27
S	85.9%	0.86	0.74	0.34	0.40
W	82.8%	0.83	0.69	0.36	0.33
N	70.7%	0.74	0.53	0.37	0.16
C	72.4%	0.84	0.61	0.38	0.23

* APSP stands for Accuracy from Primitive Sequence Prediction.

Tests were conducted at time intervals including January—December, 1999, January—July, 2000 and January—December, 1999, January 1999—July 2000 and January 1999—December 2000 as independent samples, resulting in correlation coefficients between predicted and measured values. As shown in Fig. 6, the predictions become increasingly poorer as the time intervals are prolonged for all the patterns.

3. *Comparison and Assessment*

For assumed operational purposes we employed the monthly sequences covering January 1965—December 2000 (total of 36 years or 432 months) to pinpoint mean anomaly of monthly rainfall for January—December 2001 in the context of the pattern-specific SSA-AR model (see Fig. 7).

The prognostic trends display that the wet-period rainfall amounts are below monthly mean to varying degree, a result that is basically in concord with measurements. Stated another way, the SSA-AR model based on data prior to December 2000 produces fairly good prediction of monthly rainfall, at least as regards the trends, for these patterns, indicating higher hit rates, especially in the Central, Southern and Eastern Patterns, for which predictions agree with measurements, particularly on the anomaly trends except for some difference in phase. In contrast, predictions are poorer for the Northern and Western Patterns because of unsteady rainfall and other factors. On the whole, the anomaly trends

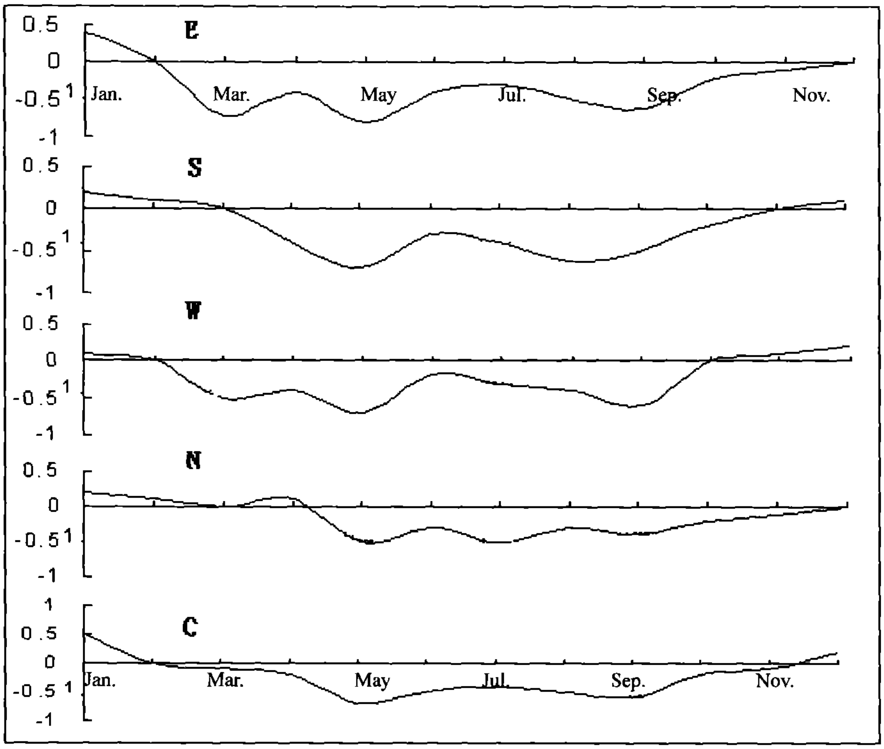

Fig. 7. SSA-AR predicted monthly rainfall for January—December 2001 in these patterns.

agree with measurements, differing only in intensity and phase for some of the patterns. The cause is that the SSA-AR scheme is for synthetic prediction based on reconstruction of component series so that the prediction accuracy depends on the quality of RC series. Examination of sub-component sequences RCs 1 — 8 given predictions reveals that they differ in quality and robustness, thereby influencing the prediction quality of the superimposed component, which is related to the prediction quality. It follows that based on the SSA decomposition, how to get RCs in an objective way and to develop a still more effective scheme are a key link of the problem.

VI. CONCLUDING REMARKS

From the foregoing study we come to the following.

(1) The annual rainfall patterns consist of three dominant types of spatial anomaly based on the LV fields (Figs. 1 — 3, viz., the pattern (i) of positive LV1 values throughout, (ii) northern positive-southern negative LV2 values and (iii) western positive-eastern positive LV3 values. North China rainfall has a key link of the change for the whole region, that is, precipitation over the central part plays a critical role in flood/drought happening throughout North China. Moreover, rainfall difference arises there owing to geographic latitude, landform and affecting systems and the opposites of flood and drought occurrence are exhibited largely in patterns (ii) and (iii).

(2) The anomalies of monthly rainfall are divided into 5 patterns, i.e., the Eastern, Southern, Western, Northern and Central, and rainfall is relatively comparable inside

each.

(3) The precipitation inside the patterns shows three leading periods, i.e., quasi 2-, quasi 4—5- or 7—8- and quasi 3-year oscillations. For the Southern, Western and Central Patterns the dominant periods are in such an order as quasi 2-, quasi 4—5- or quasi 7—8- and quasi 3-year oscillations; for the Western Pattern as quasi 2-, quasi 3- and quasi 7—8-year oscillations and just the opposite to the Western happens in the Eastern Pattern.

(4) The SSA-AR model is applicable to rainfall predicting for all the patterns. It has the following merits: (i) because SSA treatment has the same effect as a low-pass filter is used of primitive series such that high-frequency noise is removed and so are aperiodic weak signals, leading to the fact that each of the RC sequences contains one kind of wave pattern as signal so as to improve predictability, and (ii) SSA-reconstructed series RCs are not on an orthogonal base function given in advance but the typical wave vectors are extracted from series-contained wave characteristics and a superimposed sequence is equivalent to an adaptively filtered series and marked by time-dependent behaviors.

(5) The RCs of adaptively filtered series retain strong signals of the same class and exhibit dominantly temporally-varying behaviors of rainfall signal in superimposed sequences and, in addition, it is built on lower orders and marked by higher predictability and steady prediction skill.

(6) The SSA-AR scheme, if further improved in every aspect, is expected to be used as an objective county-level rainfall predicting model run automatically, which is expected to be applied on an operational basis.

REFERENCES

Chen Juying (1991), *Analysis of Floods/Droughts of China and Study on Their Long-Term Prediction*, China Agricultural Press, Beijing (in Chinese).

Ding Yuguo et al. (1998a), Experiments on short-range climate prediction of Nino-region SSTA, *Quart. Trop. Meteor.*, **14**(4): 289—296 (in Chinese).

Ding Yuguo et al. (1998b), Generalization and applications of singular spectral analysis, *Acta Meteor. Sinica*, **56**(6): 736—745 (in Chinese).

Hebei Meteorological Bureau (ed.) (1990), *Handbook of Forecasters*, China Meteor. Press, Beijing, pp. 113—116 (in Chinese).

Huang Jiayou (1988a), Analysis by rotated principal components and the application to weather/climate research, *Meteor. Monthly*, **14**(9): 47—51 (in Chinese).

Huang Jiayou (1988b), Behaviors of quasi—2 year periods in monthly rainfall of China, *Acta Scientia Atmospherica*, **12**(3): 267—273 (in Chinese).

Huang Jiayou (1991), Analysis of space/time features of summer temperature and rainfall fields in China, *Acta Scientia Atmospherica*, **15**(3): 124—132 (in Chinese).

Li Chongyin (1992), A case study of wet-period rainfall over North China, *Acta Meteor. Sinica*, **50**(1): 41—49 (in Chinese).

Li Dongliang et al. (1997), Summer rainfall characteristics with its anomaly for NW China, *Acta Scientia Atmospherica*, **21**(3): 331—340 (in Chinese).

Priestley, M. B. (1981), *Spectral Analysis and Time Series*, Academic Press, London, pp. 222—226.

Shi Neng (1995), *Multivariant Analysis Methods Used in Meteorological Research and Prediction*, China Meteor. Press, Beijing, 170 pp. (in Chinese).

Sun Li et al. (2000). Climate analysis of summer rainfall anomaly for northeastern China. *Acta Meteor. Sinica*. **58** (1): 70—81 (in Chinese).

Tang Zhongxin et al. (1990). *Analysis of Historical Records of Floods/Droughts and Cold/Warm Events over the River Haihe Valleys*. China Meteor. Press. Beijing. pp. 47—50 (in Chinese).

Vautard, S. S. A. (1992). A toolkit for noise chaotic signals. *Physics* D. **58**: 95—126.

Zhang Mingli (1993). History of rainfall in the east part of China over the past century. *Acta Scientia Atmospherica*. **17** (4): 451—461 (in Chinese).